DIAPH3 is upregulated in high-grade gliomas and linked to chromosomal instability

Caren Jabbour, Mathilde Beka, Philippe Gailly, Nicolas Tajeddine

Laboratory of Cell Physiology, Institute of Neuroscience, Université catholique de Louvain, Brussels, Belgium

Correspondence to:

Nicolas Tajeddine

Institute of Neuroscience, Université catholique de Louvain

avenue Mounier, B1.53.17

B-1200 Brussels

Phone number: + 32 2 764 55 46

Email: nicolas.tajeddine@uclouvain.be

Running title: Diaph3 expression in gliomas

Total word count: 4,187

Abstract

Background: DIAPH3 is a member of the formin family, a group of proteins that regulate actin and microtubule dynamics. During mitosis, DIAPH3 localizes specifically to the centrosome. Its loss destabilizes microtubules and disrupts mitotic spindle polarity, leading to multipolar mitoses and abnormal chromosome segregation, which ultimately causes aneuploidy in daughter cells.

Methods: We investigated *DIAPH3* expression in glioma samples – including low-grade high-grade gliomas – using publicly available datasets (TCGA and a single-cell RNA-seq study). We also explored the impact of *DIAPH3* expression on aneuploidy in cultured glioblastoma cells.

Results: *DIAPH3* expression was specifically increased in grade 4 gliomas. However, its prognostic value did not surpass that of the WHO CNS5 glioma classification. *DIAPH3* was predominantly expressed in mitotic cells and showed strong co-expression with genes involved in cell division, particularly those regulating mitotic progression and chromosome segregation. Several transcription factors known to drive proliferation and cancer progression may regulate *DIAPH3* expression. In glioblastoma cell lines, we confirmed that DIAPH3 is upregulated during mitosis, and that its knockdown increases aneuploidy.

Conclusions: These findings confirm the role of DIAPH3 in chromosome segregation in clinical glioma samples and demonstrate its association with high-grade, poor-prognosis gliomas.

Keywords: DIAPH3, gliomas, aneuploidy, chromosome segregation

Key points

- Bioinformatics analysis of publicly available databases shows that *DIAPH3* is overexpressed in high-grade gliomas.
- The expression of *DIAPH3* is correlated with that of genes involved in chromosome segregation.
- DIAPH3 repression increases aneuploidy in glioblastoma cells.

Importance of the study

The role of DIAPH3 in mitosis has so far been demonstrated only in cell lines and mouse models. By analyzing human glioma samples using integrative bioinformatics, this study provides evidence supporting its involvement in chromosome segregation in human tumors. *DIAPH3* expression is strongly correlated with genes essential for karyokinesis, predominantly observed in mitotic cells, and appears regulated by transcription factors known to control mitotic progression. These findings suggest that DIAPH3 is part of a broader mitotic transcriptional program in gliomas. Importantly, we confirm that this association reflects a causal relationship: DIAPH3 repression in glioblastoma cells increases aneuploidy, reinforcing its role in maintaining chromosomal stability. Finally, we show that *DIAPH3* is overexpressed in high-grade gliomas, linking its deregulation to tumor aggressiveness. Altogether, this study bridges experimental and clinical observations and highlights DIAPH3 as a potential biomarker and contributor to chromosomal instability in malignant gliomas.

Introduction

Diaphanous-related formin 3 (DIAPH3, also known as mDia2) belongs to the formins, a family of dimeric multidomain proteins conserved in fungi, plants and animals. All members of the formin family share a specific domain called formin homology domain 2 (FH2), which confers to these proteins their actin polymerization activity.[1] The activity of DIAPH3, like that of other DIAPH subfamily members, is inhibited by the interaction between its diaphanous autoinhibitory domain (DAD) and its DAD interacting domain (DID). This interaction is disrupted following activation of a small GTPase to the GTPase binding domain which allows the FH2 domain to access monomeric actin and polymerize it.[2]

Given their role in actin nucleation and elongation, formins are best known to be involved in cytoskeletal remodeling, cell adhesion and migration. It is therefore not surprising that formins also play a role in cancer progression.

However, studies evaluating the role of DIAPH3 in cancer have reported conflicting results. For example, depletion of DIAPH3 induces an epithelial-to-mesenchymal transition in breast, prostate and hepatocellular carcinomas, which notably promotes cell migration and metastatic spreading.[3-6] In contrast, a recent study showed that repression of DIAPH3 reduced the migration of breast cancer cells stimulated by overexpression of MRTF1, a regulator of the expression of genes relevant to cytoskeleton organization. [7] Similarly, another study showed that repressing DIAPH3 suppressed proliferation and metastatic spread in osteosarcoma.[8]

In glioblastoma (GBM) cell models, it has been shown that pharmacological activation of DIAPH3, which removes auto-inhibition, or its siRNA-mediated depletion reduced invasion and resulted in cells adopting a more epithelial-like morphology.[9,10]

The prognostic significance of *DIAPH3* expression in GBM remains controversial. While a previous study failed to establish a clear association with patient outcome, our recent analysis of a cohort of 73 GBM patients revealed that high *DIAPH3* expression correlated with improved overall survival (overall survival was 20.2 months in *DIAPH3*^{high} group *vs.* 11.7 months in *DIAPH3*^{low} group).[11,12]

DIAPH3 is also required for mitosis. It accumulates in the cleavage furrow during cytokinesis, and its depletion in dividing cells affects the quantity of F-actin in the equatorial region.[13,14] In *DIAPH3*-deficient mice, erythropoiesis is impaired because erythroid cells fail to complete cytokinesis, due to reduced actin accumulation at the cleavage furrow.[15]

In addition to its role in the dynamics of the actin cytoskeleton, DIAPH3 is also able to directly bind and stabilize microtubules (MTs) and its overexpression is sufficient to generate and orient stable MTs.[16,17]

DIAPH3 deletion in mouse neural progenitor cells impaired the activation of the spindle assembly checkpoint (SAC), which monitors the connections between spindle MTs and kinetochores and ensures the balanced segregation of chromosomes during mitosis, this leading to aneuploidy and apoptosis.[18] Moreover, DIAPH3 localizes at the centrosome during mitosis and is required for the proper organization of the mitotic spindle.[19]

DIAPH3 may therefore influence cancer progression by affecting cytoskeletal remodeling, mitotic spindle function, and chromosome segregation. The multiple effects of DIAPH3 on processes essential for the proliferation and spread of tumor cells could potentially lead to seemingly conflicting data on the effect of DIAPH3 expression on cancer prognosis.

In an attempt to understand the role of DIAPH3 in gliomas, we analyzed its expression in transcriptomic datasets from healthy and tumor tissues. We examined genes with expression patterns similar to DIAPH3 to infer its potential cellular functions, and

investigated the transcriptional mechanisms regulating its expression. We also tried to understand the mechanisms of *DIAPH3* expression.

We demonstrated that *DIAPH3* is highly expressed in high-grade gliomas compared to both normal brain tissue and low-grade gliomas. Its expression is predominantly observed in dividing cells and correlates with that of genes involved in chromosome segregation. Transcriptional regulation of *DIAPH3* appears to be mediated by several transcription factors (TF) associated with cell cycle progression and mitosis. In U251-MG GBM cells, we confirmed that DIAPH3 expression increases during mitosis, and that its knockdown increases aneuploidy.

Material and Methods

Datasets

Expression and methylation data were obtained from The Genotype-Tissue Expression (GTEx) Portal, The Cancer Genome Atlas (TCGA) Program, and the datasets GSE182109 and GSE123678 from the NCBI-GEO database. TCGA-LGG and TCGA-GBM samples were reclassified according to the 5th edition of the WHO Classification of Tumours of the Central Nervous System (WHO CNS5).[20] The table used for this reclassification is publicly available as Supplementary Table S2 in the following publication: https://www.mdpi.com/article/10.3390/ijms24010157/s1.[21]

Software and computing

All data analyses were performed using R software version 4.4.1 (2024-06-14) and GraphPad Prism version 10.4.0. Some of the steps involved in processing the single cell RNA sequencing (scRNA-seq) data from dataset GSE182109, which required large amounts of computing resources, were carried out using R software version 4.2.0 (2022-

04-22) running on a high-performance computing cluster with 1,536 cores (30 AMD Epyc Naples and 32 Intel Sandy Bridge compute nodes). The R codes were written with the help of ChatGPT-4o (OpenAI, San Francisco, CA, USA).

Comparison of DIAPH3 expression in normal and tumor tissues

To compare DIAPH3 expression data in GTEx normal tissue and TCGA tumor tissue, expression and phenotypic data, including tissue type, were retrieved from the UCSC Xena platform (gtex_RSEM_Hugo_norm_count.gz and TcgaTargetGtex_RSEM_Hugo_norm_count.gz datasets) with the UCSCXenaTools package.[22]

Extraction of expression and clinical data from TCGA

Transcriptomic and clinical data from TCGA-LGG and TCGA-GBM cohorts were accessed via the TCGAbiolinks R package. Gene expression data were queried, downloaded, and prepared through a standardized workflow, including preprocessing based on correlation filtering, normalization using the "gcContent" method, and quantile-based filtering.[23,24] Clinical data were separately retrieved for each project, combined, and filtered to include only primary tumor samples.

Survival analysis

Survival data were matched to DIAPH3 expression levels. For each subgroup – all gliomas combined, low-grade, and high-grade gliomas – samples were dichotomized into high- and low-expression groups based on the median DIAPH3 expression specific to that subgroup. Kaplan-Meier survival curves and associated statistical analyses were then performed using GraphPad Prism.

Gene ontology (GO) enrichment

GO enrichment analyses were conducted to identify Biological Processes (BP), Cellular Components (CC), and Molecular Functions (MF) associated with genes showing significant Pearson correlation with DIAPH3 expression in the TCGA-LGG and TCGA-GBM cohorts. GO enrichment analysis was performed using the gseGO function from the clusterProfiler package, with a minimum gene set size of 100, a maximum of 500, and a p-value cutoff of 0.05.[25] Only positively regulated pathways were retained for further analysis.

Analysis of scRNA-seq data

The scRNA-seq data from the GSE182109 study were analyzed to identify cell type-specific expression patterns and perform GO enrichment analysis. Raw expression data from 10X Genomics were processed for each sample using the Seurat R package, with cells filtered based on mitochondrial content (>25%) and gene feature counts (200–9000).[26] Predicted cell types were annotated using the scATOMIC R package and cell cycle phases were scored using predefined S and G2/M gene sets.[27] To infer the CNV status of individual cells, we employed the CNV mode of scATOMIC, which utilizes CopyKAT for CNV inference. This approach allowed to classify cells as either diploid or aneuploid based on their inferred CNV profiles. The processed data were normalized, variable features identified and scaled to regress out cell cycle effects. All samples were integrated into a single Seurat object, and dimensionality reduction (PCA and UMAP) and clustering (resolution = 0.1) were performed. Analysis of GO enrichment was carried out as described above.

Analysis of DIAPH3 promoter methylation

DNA methylation profiles from TCGA-LGG and TCGA-GBM cohorts were analyzed using data from the Illumina HumanMethylation450k array to investigate methylation patterns in a genomic region spanning *DIAPH3* on chromosome 13. Data Annotation information for the 450k platform was obtained using the IlluminaHumanMethylation450kanno.ilmn12.hg19 package. Probes located within a 1 kb region upstream of *DIAPH3* were identified. Methylation beta-values for these probes were retrieved from the GDC portal using the TCGAbiolinks R package and filtered to include only primary tumor samples.

Similarly, DNA methylation data and clinical data from the GSE123678 dataset were retrieved from the NCBI-GEO database. Annotation and filtering steps mirrored those used for the TCGA data.

TF binding motif analysis

TF binding motif analysis was performed on genes significantly correlated with *DIAPH3* expression (Pearson correlation > 0.5) using the RcisTarget R package.[28] Motif rankings were retrieved from the hg38_10kbp_up_10kbp_down_full_tx_v10_clust database, and enrichment analysis was conducted to identify TF motifs with a normalized enrichment score (NES) > 3. Position Weight Matrices (PWMs) for the identified TFs were obtained from the JASPAR2022 database, and their binding sites were mapped onto the putative *DIAPH3* promoter region (~1000 bp upstream of the transcription start site, TSS) using the searchSeq function from the TFBSTools package.[29] Conservation scores for this region were imported from the UCSC hg38 phastCons20way track and used to assess the evolutionary conservation of TF binding sites.

ChIP-seq-based identification of TF binding sites

To identify TFs binding to the putative *DIAPH3* promoter region, we analyzed ChIP-seq peak data from the ReMap2022 database. TF-specific BED files were obtained and processed using the R packages GenomicRanges, and rtracklayer. Each BED file was imported as a GRanges object and annotated with the corresponding TF name. All entries were concatenated into a single GRanges object and filtered for overlaps with a ±1000 bp window downstream of the DIAPH3 TSS. Only peaks with a ReMap score above 50 and detected in selected cell lines (K-562, Hep-G2, HEK293, or U266B1) were retained. When multiple peaks were found for the same TF, only the highest-scoring peak was kept.

Cell culture

U251-MG glioblastoma cells (harboring the $p53^{R273H}$ mutation) were cultured in Dulbecco's Modified Eagle Medium (DMEM, Gibco) supplemented with 10% fetal bovine serum (FBS). Cells were maintained at 37 °C in a humidified atmosphere containing 5% CO_2. The U251-MG cells used in this study were authenticated by Multiplexion GmbH (Friedrichshafen, Germany) using the Multiplex Cell Authentication assay. The analysis confirmed a 100% identity with the U251-MG reference profile and excluded cross-contamination with other human cell lines.

Cell transfection

U251-MG cells were transfected for 72 hours with a pool of four siRNAs targeting DIAPH3 (ON-TARGETplus Human DIAPH3 siRNA SMARTpool, Dharmacon), using DharmaFECT 1 transfection reagent (Dharmacon), following the manufacturer's instructions. A non-targeting siRNA pool (ON-TARGETplus Non-targeting Control siRNA, Dharmacon) was used as a negative control.

Immunoblotting

Cells were harvested and lysed in RIPA buffer (50 mM Tris–HCl, pH 7.6; 150 mM NaCl; 1% Triton X-100; 0.5% sodium deoxycholate; 0.1% SDS; 1 mM EDTA). Equal amounts of protein were resolved on 4–20% Mini-PROTEAN TGX precast gels (Bio-Rad) and transferred to PVDF membranes. Membranes were blocked with 5% non-fat dry milk or bovine serum albumin (BSA) in TBS-T (TBS with 0.1% Tween-20), then incubated overnight at 4 °C with the following primary antibodies diluted in blocking buffer: rabbit polyclonal anti-DIAPH3 (Abcam, #AB245660; 1:2500), rabbit polyclonal anti-phospho-Histone H3 (Cell Signaling Technology, #3377; 1:1000) and rabbit monoclonal anti-GAPDH (Cell Signaling Technology, #2118; 1:10000). After washing, membranes were incubated for 1 hour at room temperature with HRP-conjugated goat anti-rabbit secondary antibody (Dako). Signal was detected using enhanced chemiluminescence (Fusion Pulse system), and band intensities were quantified using the "Gel Analyzer" tool in Fiji (ImageJ).

Isolation of mitotic and interphase U251-MG cells

To isolate mitotic cells, U251-MG GBM cells were cultured under standard conditions and subjected to a single mechanical shake-off. Culture flasks were firmly tapped to selectively detach rounded mitotic cells, which were immediately collected from the supernatant. Adherent cells remaining attached to the culture surface (predominantly interphase cells) were then harvested by gentle scraping in cold PBS. Both mitotic and adherent cell fractions were lysed separately and processed for protein extraction followed by immunoblot analysis.

Metaphase spread

Cells were treated with 0.05 µg/mL colcemid for 3 hours to arrest cells in metaphase. They were then collected by centrifugation at 1,000 rpm for 5 minutes, incubated in hypotonic solution (0.065M KCl in distilled water), and fixed in methanol:acetic acid (3:1). Metaphase spreads were prepared by dropping the fixed cell suspension onto clean microscope slides. Slides were stained with Wright stain diluted in phosphate buffer and examined under a 100× oil immersion objective using an Axiovert 200 M microscope (Zeiss, Germany).

Code availability

All codes are available at https://github.com/NTajeddine/Jabbour_et_al_2025.

Results

DIAPH3 is overexpressed in high-grade gliomas and transcriptionally regulated by proliferation-linked factors

Expression data from the GTEx project show that *DIAPH3* expression in normal tissues is highest in bone marrow and testis (Fig. 1A). In contrast, expression is low in tissues such as muscle where there is little cell division.

Based on expression data from GTEx and TCGA project, *DIAPH3* expression is significantly higher in tumour tissues compared to normal tissues (Fig. 1B).

As *DIAPH3* expression is similar in grade 4 astrocytomas and GBM, these samples were grouped under the name CNS5-HGG (high-grade gliomas) (Fig. S1). Grade 2 and grade 3 gliomas are grouped together as CNS5-LGG (low-grade gliomas).

The expression of *DIAPH3* is similar in normal brain tissue and CNS5-LGG samples. However, it increases significantly in CNS5-HGG samples (Fig. 1C). Mutations in the *DIAPH3* gene are very rare (less than 1%) in TCGA samples from gliomas.

Using the UCSC Genome Browser, we identified a region of high TFs binding site density in the ReMap Density track, extending up to 1,000 base pairs upstream of the *DIAPH3* transcription start site (TSS). Based on this observation, we focused our analyses on this promoter-proximal region to assess DNA methylation patterns and to identify candidate TFs potentially involved in the regulation of *DIAPH3* expression.

Analysis of TCGA glioma samples revealed that this region is consistently hypomethylated, with no correlation observed between its methylation levels and DIAPH3 expression (Fig. S2A). We confirmed this finding using data from the GSE123678 dataset, which includes both normal brain and glioma samples.[30] Again, methylation was very low and did not differ significantly between normal and tumor samples (Fig. S2B).

We next applied the RcisTarget package to identify TFs that may regulate genes co-expressed with *DIAPH3* in TCGA gliomas samples. We then searched for binding motifs of these candidate TFs within the 1,000 bp region upstream of the *DIAPH3* TSS (Fig. 1D). Several TFs identified in this region are known regulators of the cell cycle, including TFDP1, SP2, E2F6, E2F8, and members of the NF-Y complex. Their presence suggests that *DIAPH3* expression may be tightly coupled to cell cycle control. In addition, TFs such as HOXA2, HOXB2, FOXI1, and IRF6, which are involved in developmental and differentiation processes, were also identified.

Finally, we interrogated the ReMap2022 database to determine whether binding of these transcription factors to the upstream region of DIAPH3 has been experimentally demonstrated by ChIP-seq. The ChIP-seq data indicate transcription factor occupancy of the 1,000 bp region upstream of the DIAPH3 transcription start site (TSS) by TFDP1, SP2,

E2F8, and members of the NF-Y family, consistent with their potential involvement in the transcriptional regulation of DIAPH3, although these data do not distinguish between direct DNA binding and indirect association through protein–protein interactions.

Prognostic impact of DIAPH3 expression in TCGA gliomas stratified by WHO CNS5 classification

In the TCGA data, we analysed the association of *DIAPH3* with survival in patients with CNS5-LGG or CNS5-HGG. High *DIAPH3* expression, defined as above the cohort median, is associated with a poor prognosis when considering all gliomas, with median survival decreasing from 107 months in the *DIAPH3* low group to 22 months in the *DIAPH3* high group (Fig. 2A). However, this association is no longer observed when CNS5-LGG and CNS5-HGG samples are analysed separately (Fig. 2B and 2C, respectively). This indicates that *DIAPH3* expression does not provide additional prognostic value beyond the CNS5 classification as a prognostic marker.

Proteins involved in karyokinesis, post-translational modifications and the formation of the extracellular matrix show an expression profile like that of DIAPH3

To determine the role of DIAPH3 in gliomas, we compiled a list of genes whose expression is similar to that of *DIAPH3* in TCGA gliomas patients. The list of these genes and their correlation coefficient with *DIAPH3* expression is shown in Supplementary Table S1.

We then studied the processes in which these genes were involved by performing gene enrichment analyses in the GO knowledgebase.

Genes expressed in a similar way to *DIAPH3* are involved in biological processes relating to mitosis and, in particular, DNA replication, karyokinesis and chromosome segregation (Fig. 3A). These include the *CENPE*, *KIF18A*, *KIF23* and *SKA3* genes (Fig. 3B). *BORA*, *BUB1*

and *PLK1* which encode proteins that ensure and control the attachment of kinetochores to microtubules during metaphase, also show an expression profile similar to that of *DIAPH3*.

As expected, the cellular components that are over-represented in the list of genes that have similar expression to *DIAPH3* in gliomas are related to chromosomes, centromeric regions and the mitotic spindle (Fig. 3C). More surprisingly, a group of genes encoding proteins associated with the endoplasmic reticulum were also found. These proteins include glycosyltransferases (*DDOST*, *POGLUT3*, *RPN2*) and disulphide isomerases (*P4HB*, *PDIA4*, *PDIA6*).

Genes expressed as *DIAPH3* were enriched for molecular functions associated with isomerase, glycosyl- and hexosyltransferase activities and DNA binding and DNA modification (Fig. 3E). This is consistent with the biological processes and cellular components identified previously. A significant number of genes encoding proteins known to be constituents of the extracellular matrix also show similar expression to *DIAPH3*. Of these, those with the highest correlation with *DIAPH3* expression were *COL21A1*, *EFEMP2*, *HSPG2*, *LAMB1* and *LAMC1* (Fig. 3F).

DIAPH3 is mainly expressed in dividing GBM cells

To study how *DIAPH3* was expressed within the cells that constitute GBM tumor masses, we analyzed expression in scRNA-seq data. To do this, we used the GSE182109 study which sequenced a total of 201,986 cells from 44 samples from 18 GBM patients.[31] *DIAPH3* was expressed in ~6% of all cells (Fig. 4A). Approximately 10% of gliomas cells expressed *DIAPH3*. *DIAPH3* was also expressed in stromal cells (~14%) and, to a much lesser extent, in blood cells (~2%).

In GBM cells, *DIAPH3* expression was clearly predominant in cells undergoing mitosis, with 30% of G2/M cells expressing *DIAPH3* as compared with only 3% of G0/G1 cells (Fig. 4B).

As with the TCGA samples, we compiled a list of genes whose expression was similar to that of *DIAPH3* (Supplementary Table 2). However, we limited this analysis to GBM cells in G2/M phase (~6000 cells). We then performed GO enrichment on this list. For all three ontologies, we found processes associated with mitosis and, more specifically, with chromosome segregation (Fig. 4C, D and E).

Contrary to what was observed in the TCGA bulk RNAseq data, the expression of glycosyltransferases, disulfide isomerases and extracellular matrix components was not associated with that of *DIAPH3* in GBM cells in the GSE182109 study.

Aneuploidy is correlated with DIAPH3 expression

Since our own experimental data show that DIAPH3 is involved in SAC function and GO enrichment data suggest that DIAPH3 is involved in correct chromosome segregation during mitosis, we analyzed aneuploidy in TCGA glioma samples as a function of DIAPH3 expression. Surprisingly, the aneuploidy score was significantly higher in samples where *DIAPH3* expression was higher than the median (Figure 5). Similar results were obtained for other genes known to be involved in SAC (*BUB1*, *BUB1B*, *MAD2L2*). Only *MAD1L1* expression was inversely correlated with the aneuploidy score.

We also analyzed *DIAPH3* expression in GBM cells from dataset GSE182109. Chi-squared analysis showed that *DIAPH3* was expressed more frequently in aneuploid cells than in diploid cells (Fig. S3).

DIAPH3 knockdown induces aneuploidy in GBM cells

To complement our bioinformatic analyses of DIAPH3 expression in glioma patient datasets, we performed in vitro experiments using human GBM cells. In U251-MG cells, a well-characterized GBM cell line, we observed that DIAPH3 is highly expressed and that its expression increases during mitosis (Fig. 6A and 6B).

To investigate whether changes in *DIAPH3* expression are merely correlated with aneuploidy or may actively contribute to it, we silenced DIAPH3 using a pool of siRNAs in U251-MG cells and examined chromosome numbers in metaphase cells. Immunoblotting confirmed that the siRNA pool efficiently reduced DIAPH3 expression (Fig. 6C). As anticipated, the median chromosome number per cell remained unchanged following DIAPH3 knockdown. However, the distribution of chromosome numbers was significantly broader in DIAPH3-silenced cells, indicating increased variability in chromosome segregation and suggesting a rise in aneuploidy (Fig. 6D and 6E).

Discussion

The most striking finding of this bioinformatics analysis is that high DIAPH3 expression is specifically associated with high-grade gliomas, as its expression levels are comparable between normal brain tissue and low-grade gliomas. Interestingly, using an optimal DIAPH3 expression cutoff of 6.7 ($\log_2$(normalized counts + 1)) determined by ROC analysis, we achieved a sensitivity of 85.7% and a specificity of 80.2% in distinguishing CNS5-HGG from CNS5-LGG. These results suggest that DIAPH3 could represent a useful biomarker for differentiating low-grade from high-grade gliomas. Moreover, because its expression appears to be largely restricted to high-grade gliomas, DIAPH3 may also represent a potential therapeutic target whose selective expression pattern could offer opportunities for tumor-specific intervention.

One possible explanation for the selective overexpression of *DIAPH3* in high-grade gliomas is its association with *IDH* status. Indeed, the vast majority of gliomas classified as grade 4 according to the WHO CNS5 criteria are *IDH*-wild type. *IDH* mutation induces the formation of D-2-hydroxyglutarate, a competitive inhibitor of TET, which is an activator of DNA demethylation.[32] *IDH* mutation is therefore associated with DNA hypermethylation and a better prognosis, notably in gliomas. It could therefore be hypothesized that if DIAPH3 is more highly expressed in *IDH*-wild type gliomas, it is because its promoter is demethylated. However, our analyses show that the *DIAPH3* promoter is only slightly methylated and that its methylation level does not change significantly between normal brain tissue and gliomas.

If DIAPH3 is involved in the normal functioning of the spindle assembly checkpoint, the fact that it is expressed in high-grade gliomas, and therefore associated with a poor prognosis, may seem surprising. One might expect that reducing DIAPH3 expression by altering the SAC would increase aneuploidy and reduce tumour aggressiveness. However, this is not the case. On the contrary, the more DIAPH3 is expressed, the higher the aneuploidy score in gliomas. The same observation is made for the expression of other genes coding for proteins whose role in SAC is well established. An obvious explanation for this apparent contradiction is that overexpression of certain SAC proteins in tumor cells may be a consequence rather than a cause of SAC failure. It is also plausible that both overexpression and underexpression of these proteins disrupt the delicate balance required for proper kinetochore function and accurate chromosome segregation, thereby increasing the risk of aneuploidy. Indeed, both overexpression and underexpression of SAC proteins disturb mitotic fidelity.[33] Our *in vitro* findings indicate that repression of DIAPH3 increases aneuploidy in GBM cells. This suggests that changes in DIAPH3 expression not only correlate with aneuploidy but may also cause it.

It should be noted that the frequency of *DIAPH3* mutation in cancers is very low (less than 2% of all TCGA samples) and there is no difference between the aneuploidy scores of samples with wild-type or mutated *DIAPH3*. It can therefore be concluded that neither low *DIAPH3* expression nor *DIAPH3* mutation is the cause of increased aneuploidy in tumor cells.

The significance of aneuploidy in cancer cells is complex and not fully understood.[34] Aneuploidy is often found in cancer cells, where it is thought to favor cancer initiation or progression.[35] The ability of cancer cells to resist senescence inducers or proapoptotic signals is thought to allow aneuploid cells to survive and proliferate.[36] By promoting genomic instability, aneuploidy may also facilitate genomic mutations leading to tumor heterogeneity and conferring phenotypic adaptations to cancer cells in the absence of growth factors or nutrients or in the presence of cytotoxic insults such as chemotherapy or radiation.[37] In contrast, exacerbating aneuploidy in cancer cells by destabilizing the SAC may lead to tumor suppression through the induction of cell death.[38,39] Aneuploidy may also favor the induction of mitotic catastrophe by drugs that interfere with chromosome segregation.[40,41]

The key pathway consistently enriched in all GO analyses, regardless of dataset (TCGA or scRNA-seq) or ontology, is cell division, in particular mitotic progression and chromosome segregation. Genes positively correlated with *DIAPH3* expression are associated with mitotic nuclear division, sister chromatid segregation and DNA replication. This strongly suggests that the observations made on the role of *DIAPH3* in SAC function in cell and mouse models can be extrapolated to glioma patients. This also explains why *DIAPH3* is mainly expressed in tissues where mitotic activity is intense, such as bone marrow, testis and cancers.

Our analysis revealed that several TFs – TFDP1, E2F8, SP2, and the NF-Y complex – bind to the putative *DIAPH3* promoter region, as confirmed by ChIP-seq data from the ReMap2022 database. All are known regulators of cell cycle genes and have established roles in cancer. TFDP1 forms heterodimers with E2F TFs to regulate genes involved in the G1/S transition and mitotic progression. Both TFDP1 and E2F8 have been linked to increased proliferation and poor prognosis in several malignancies, including GBM.[42-44] SP2, although less studied, belongs to SP protein family, which is involved in the regulation of cell proliferation, differentiation and apoptosis.[45] It is associated with a poor prognosis in hepatocellular carcinoma.[46] The NF-Y complex regulates genes involved in DNA replication and mitosis. Overexpression of NF-Y – mostly *NFYA* – is oncogenic and decreases sensitivity to anti-neoplastic drugs.[47] Together, these findings support the hypothesis that *DIAPH3* is integrated into a transcriptional network controlling mitosis and cell proliferation – pathways commonly hijacked in cancer – and suggest a functional role for DIAPH3 in glioma progression and chromosomal instability.

A fundamental limitation of retrospective studies on clinical data is their inability to establish causal relationships, as they can only reveal correlations. Nevertheless, the strength of the present study lies in its strong indication that the effects of DIAPH3 on proper chromosome segregation, previously observed in cellular and animal models, may also extend to glioma patients.

Further investigations in preclinical models will be essential to elucidate the mechanisms by which DIAPH3 contributes to SAC control and to assess its potential as a therapeutic target for glioma treatment.

Required Statements

Ethics. This study does not involve animal testing. Patient data were obtained from public databases.

Funding. This work was supported by the Fonds spéciaux de Recherche of UCLouvain (FSR2022 and FSR2024) and the Fonds de la Recherche scientifique - FNRS (Grants J.0182.22 and J.0201.24).

Conflict of Interest. The authors have no relevant financial or non-financial interests to disclose.

Authorship. CJ, PG and NT designed and concepted the study and wrote the codes and the paper. CJ and MB designed and conducted the *in vitro* experiments.

Data availability. All the data used in this study are accessible on public databases, the web links to which are given in the Material and Methods section. The R codes used to process these data are available at https://github.com/NTajeddine/Jabbour_et_al_2025. The data tables generated by these R codes are available as Excel files in additional data.

References

1. Chesarone MA, DuPage AG, Goode BL. Unleashing formins to remodel the actin and microtubule cytoskeletons. *Nat Rev Mol Cell Biol.* 2010; 11(1):62-74.
2. Alberts AS. Identification of a carboxyl-terminal diaphanous-related formin homology protein autoregulatory domain. *J Biol Chem.* 2001; 276(4):2824-2830.
3. Di Vizio D, Kim J, Hager MH, et al. Oncosome formation in prostate cancer: association with a region of frequent chromosomal deletion in metastatic disease. *Cancer Res.* 2009; 69(13):5601-5609.
4. Hager MH, Morley S, Bielenberg DR, et al. DIAPH3 governs the cellular transition to the amoeboid tumour phenotype. *EMBO Mol Med.* 2012; 4(8):743-760.
5. Morley S, You S, Pollan S, et al. Regulation of microtubule dynamics by DIAPH3 influences amoeboid tumor cell mechanics and sensitivity to taxanes. *Sci Rep.* 2015; 5:12136.
6. Su T, Zhang N, Wang T, et al. Super Enhancer-Regulated LncRNA LINC01089 Induces Alternative Splicing of DIAPH3 to Drive Hepatocellular Carcinoma Metastasis. *Cancer Res.* 2023; 83(24):4080-4094.
7. Eder I, Yu V, Antonello J, et al. mDia2 is an important mediator of MRTF-A-dependent regulation of breast cancer cell migration. *Mol Biol Cell.* 2024; 35(10):ar133.
8. Zhang Z, Dai F, Luo F, et al. Diaphanous related formin 3 knockdown suppresses cell proliferation and metastasis of osteosarcoma cells. *Discov Oncol.* 2021; 12(1):20.
9. Arden JD, Lavik KI, Rubinic KA, et al. Small-molecule agonists of mammalian Diaphanous-related (mDia) formins reveal an effective glioblastoma anti-invasion strategy. *Mol Biol Cell.* 2015; 26(21):3704-3718.
10. Heuser VD, Kiviniemi A, Lehtinen L, et al. Multiple formin proteins participate in glioblastoma migration. *BMC Cancer.* 2020; 20(1):710.

11. Chehade G, El Hajj N, Aittaleb M, et al. DIAPH3 predicts survival of patients with MGMT-methylated glioblastoma. *Front Oncol.* 2024; 14:1359652.

12. Stoyanov GS, Lyutfi E, Georgieva R, et al. Diaph3 underlines tumor cell heterogeneity in glioblastoma with implications for treatment modalities resistance. *J Neurooncol.* 2022; 157(3):523-531.

13. Watanabe S, Ando Y, Yasuda S, et al. mDia2 induces the actin scaffold for the contractile ring and stabilizes its position during cytokinesis in NIH 3T3 cells. *Mol Biol Cell.* 2008; 19(5):2328-2338.

14. Watanabe S, Okawa K, Miki T, et al. Rho and anillin-dependent control of mDia2 localization and function in cytokinesis. *Mol Biol Cell.* 2010; 21(18):3193-3204.

15. Watanabe S, De Zan T, Ishizaki T, et al. Loss of a Rho-regulated actin nucleator, mDia2, impairs cytokinesis during mouse fetal erythropoiesis. *Cell Rep.* 2013; 5(4):926-932.

16. Bartolini F, Moseley JB, Schmoranzer J, Cassimeris L, Goode BL, Gundersen GG. The formin mDia2 stabilizes microtubules independently of its actin nucleation activity. *J Cell Biol.* 2008; 181(3):523-536.

17. Palazzo AF, Cook TA, Alberts AS, Gundersen GG. mDia mediates Rho-regulated formation and orientation of stable microtubules. *Nat Cell Biol.* 2001; 3(8):723-729.

18. Damiani D, Goffinet AM, Alberts A, Tissir F. Lack of Diaph3 relaxes the spindle checkpoint causing the loss of neural progenitors. *Nat Commun.* 2016; 7:13509.

19. Lau EO, Damiani D, Chehade G, et al. DIAPH3 deficiency links microtubules to mitotic errors, defective neurogenesis, and brain dysfunction. *Elife.* 2021; 10.

20. Louis DN, Perry A, Wesseling P, et al. The 2021 WHO Classification of Tumors of the Central Nervous System: a summary. *Neuro Oncol.* 2021; 23(8):1231-1251.

21. Zakharova G, Efimov V, Raevskiy M, et al. Reclassification of TCGA Diffuse Glioma Profiles Linked to Transcriptomic, Epigenetic, Genomic and Clinical Data, According to the 2021 WHO CNS Tumor Classification. *Int J Mol Sci.* 2022; 24(1).

22. Wang S, Liu X. The UCSCXenaTools R package: a toolkit for accessing genomics data from UCSC Xena platform, from cancer multi-omics to single-cell RNA-seq. *The Journal of Open Source Software.* 2019; 4(40):1627.

23. Colaprico A, Silva TC, Olsen C, et al. TCGAbiolinks: an R/Bioconductor package for integrative analysis of TCGA data. *Nucleic Acids Res.* 2016; 44(8):e71.

24. Silva TC, Colaprico A, Olsen C, et al. TCGA Workflow: Analyze cancer genomics and epigenomics data using Bioconductor packages. *F1000Res.* 2016; 5:1542.

25. Xu S, Hu E, Cai Y, et al. Using clusterProfiler to characterize multiomics data. *Nat Protoc.* 2024; 19(11):3292-3320.

26. Hao Y, Stuart T, Kowalski MH, et al. Dictionary learning for integrative, multimodal and scalable single-cell analysis. *Nat Biotechnol.* 2024; 42(2):293-304.

27. Nofech-Mozes I, Soave D, Awadalla P, Abelson S. Pan-cancer classification of single cells in the tumour microenvironment. *Nat Commun.* 2023; 14(1):1615.

28. Aibar S, Gonzalez-Blas CB, Moerman T, et al. SCENIC: single-cell regulatory network inference and clustering. *Nat Methods.* 2017; 14(11):1083-1086.

29. Tan G, Lenhard B. TFBSTools: an R/bioconductor package for transcription factor binding site analysis. *Bioinformatics.* 2016; 32(10):1555-1556.

30. Court F, Le Boiteux E, Fogli A, et al. Transcriptional alterations in glioma result primarily from DNA methylation-independent mechanisms. *Genome Res.* 2019; 29(10):1605-1621.

31. Abdelfattah N, Kumar P, Wang C, et al. Single-cell analysis of human glioma and immune cells identifies S100A4 as an immunotherapy target. *Nat Commun.* 2022; 13(1):767.

32. Han S, Liu Y, Cai SJ, et al. IDH mutation in glioma: molecular mechanisms and potential therapeutic targets. *Br J Cancer.* 2020; 122(11):1580-1589.

33. Hosea R, Hillary S, Naqvi S, Wu S, Kasim V. The two sides of chromosomal instability: drivers and brakes in cancer. *Signal Transduct Target Ther.* 2024; 9(1):75.

34. Sdeor E, Okada H, Saad R, Ben-Yishay T, Ben-David U. Aneuploidy as a driver of human cancer. *Nat Genet.* 2024; 56(10):2014-2026.

35. Sansregret L, Swanton C. The Role of Aneuploidy in Cancer Evolution. *Cold Spring Harb Perspect Med.* 2017; 7(1).

36. Soto M, Raaijmakers JA, Bakker B, et al. p53 Prohibits Propagation of Chromosome Segregation Errors that Produce Structural Aneuploidies. *Cell Rep.* 2017; 19(12):2423-2431.

37. Lee AJ, Endesfelder D, Rowan AJ, et al. Chromosomal instability confers intrinsic multidrug resistance. *Cancer Res.* 2011; 71(5):1858-1870.

38. Silk AD, Zasadil LM, Holland AJ, Vitre B, Cleveland DW, Weaver BA. Chromosome missegregation rate predicts whether aneuploidy will promote or suppress tumors. *Proc Natl Acad Sci U S A.* 2013; 110(44):E4134-4141.

39. Zasadil LM, Britigan EM, Ryan SD, et al. High rates of chromosome missegregation suppress tumor progression but do not inhibit tumor initiation. *Mol Biol Cell.* 2016; 27(13):1981-1989.

40. Janssen A, Kops GJ, Medema RH. Elevating the frequency of chromosome mis-segregation as a strategy to kill tumor cells. *Proc Natl Acad Sci U S A.* 2009; 106(45):19108-19113.

41. Kops GJ, Foltz DR, Cleveland DW. Lethality to human cancer cells through massive chromosome loss by inhibition of the mitotic checkpoint. *Proc Natl Acad Sci U S A.* 2004; 101(23):8699-8704.

42. Lee DY, Chun JN, Cho M, So I, Jeon JH. Emerging role of E2F8 in human cancer. *Biochim Biophys Acta Mol Basis Dis.* 2023; 1869(6):166745.

43. Ju G, Lin Q, Lu L, et al. TFDP1 drives triple-negative breast Cancer development through senescence suppression and serves as a therapeutic target for topotecan. *Int J Biol Macromol.* 2025; 310(Pt 4):143543.

44. Lu X, Lv XD, Ren YH, et al. Dysregulation of TFDP1 and of the cell cycle pathway in high-grade glioblastoma multiforme: a bioinformatic analysis. *Genet Mol Res.* 2016; 15(2).

45. Safe S. Specificity Proteins (Sp) and Cancer. *Int J Mol Sci.* 2023; 24(6).

46. Zhu Y, Cui J, Liu J, Hua W, Wei W, Sun G. Sp2 promotes invasion and metastasis of hepatocellular carcinoma by targeting TRIB3 protein. *Cancer Med.* 2020; 9(10):3592-3603.

47. Dolfini D, Gnesutta N, Mantovani R. Expression and function of NF-Y subunits in cancer. *Biochim Biophys Acta Rev Cancer.* 2024; 1879(2):189082.

Legends of the figures

Fig. 1. A *DIAPH3* expression in healthy tissue samples from The GTEx Portal. Each point represents one sample, and the bars represent the median expression. **B** Expression of DIAPH3 in healthy tissue samples from the GTEx and in tumor tissue samples from TCGA. Mann-Whitney test was used to determine statistical significance. **** $p < 0.0001$ **C** Expression of *DIAPH3* in normal brain tissue samples from the GTEx and gliomas from the TCGA restratified as grade 2, 3 or 4 according the WHO CNS5 classification. A Kruskal-Wallis One-Way ANOVA was performed. * $p < 0.05$ and **** $p < 0.0001$. **D** TF binding motifs identified in the putative promoter region of *DIAPH3* and their conservation scores. The relative positions of the motifs are shown on the x-axis, with their distance from the TSS, while the corresponding TFs are listed on the y-axis. Rectangles represent the positions of the motifs, colored according to their mean conservation scores (low to high conservation: dark blue to dark red). **E** ChIP-seq–validated TF binding sites within 1,000 bp upstream of the DIAPH3 transcription start site (TSS), based on ReMap2022 data. Only high-confidence peaks (score > 50) detected in selected cell lines (K-562, Hep-G2, HEK293, U266B1) are shown. For each TF, the most confident binding site overlapping the region is displayed.

Fig. 2. A Kaplan–Meier survival curves for overall survival in glioma patients from TCGA, stratified by DIAPH3 expression level (log-rank test). Data were censored at the time of last follow-up. **B** Same analysis as in A, restricted to TCGA glioma samples reclassified as grade 2 or 3 according to the WHO CNS5 classification (referred to as CNS5-LGG). **C** Same analysis as in A, restricted to TCGA glioma samples reclassified as grade 4 according to the WHO CNS5 classification (referred to as CNS5-HGG).

Fig. 3. A GO enrichment analyses showing the top 10 biological processes enriched in genes positively correlated with *DIAPH3* expression in glioma patients from TCGA. Each dot represents a biological process, with the size of the dot indicating the number of genes involved in the pathway (GeneRatio), and the color corresponding to the adjusted p-value. Pathways are sorted by GeneRatio, highlighting the most significant and enriched biological processes in glioma samples. **B** Top 5 genes contributing to the enrichment of the top 10 activated biological processes. The figure highlights the top 5 genes most correlated with Diaph3 expression that contribute to the enrichment of the top 10 positively activated biological processes identified in the gene set enrichment analysis. Rows represent the biological processes and columns represent the most correlated genes. Each tile indicates the involvement of a gene in a specific biological process, emphasizing their contribution to pathway activation in glioma samples. **C** The same as in A, but for the cellular components. **D** The same as in B, but for the cellular components. **E** The same as in A, but the molecular functions. **F** The same as in B, but for the molecular functions.

Fig. 4. A Percentage of cells expressing *DIAPH3* by cell type in the GSE182109 scRNA-seq study. **B** Percentage of GBM cells expressing *DIAPH3* by cell cycle phase. **C** GO enrichment analyses showing the top 10 biological processes enriched in genes positively correlated with *DIAPH3* expression in GBM cells in the G2/M phase. **D** The same as in A, but for cellular components. **E** The same as in A, but for molecular functions.

Fig. 5. Aneuploidy scores in glioma samples from TCGA as a function of the expression of *DIAPH3* and genes encoding proteins involved in SAC. The cut-off value used to determine low and high gene expression is the median expression of the gene in all the samples.

Fig. 6. A Immunoblot analysis of DIAPH3 expression in adherent cells (Adh) and in cells collected from the supernatant (SN) following mechanical detachment by tapping the culture flasks, a method used to enrich for mitotic cells. A non-specific band (indicated by an arrow) serves as a loading control. Expression of phospho-histone H3 (PHH3) confirms the enrichment of mitotic cells in the supernatant fraction. **B** Quantification of DIAPH3 expression normalized to the non-specific loading control. Data are presented as an estimation plot showing paired individual measurements, the mean difference, and its 95% confidence interval (p = 0.0015, paired t-test). **C** Immunoblot confirming DIAPH3 knockdown in U251-MG cells transfected with a pool of four siRNAs targeting DIAPH3 mRNA (siDIAPH3), compared to cells transfected with a non-targeting control pool (siCTRL). GAPDH was used as a loading control. **D** Representative metaphase spreads illustrating chromosome number counting under the indicated siRNA conditions. **E** Each dot represents the number of chromosomes counted in a single U251 cell under the indicated condition. Horizontal bars indicate median values. Statistical comparison was performed using Levene's test to assess differences in variance rather than central tendency, based on the expectation that increased aneuploidy manifests as a broader distribution of chromosome numbers without necessarily altering the median ($p < 0.01$, n = 50 cells from at least three independent experiments).

Lay Summary for NOA-D-25-00131R1

Gliomas are brain tumors that can vary in severity, and researchers are working to better understand what causes the most aggressive forms. The authors of this study wanted to look at a protein called DIAPH3, which helps cells divide properly, to see if it plays a role in glioma development. To do this, they studied DIAPH3 in public tumor datasets and lab-grown glioblastoma cells. Their study found that DIAPH3 levels were higher in the most aggressive gliomas, and that reducing this protein caused cells to divide abnormally. These findings show that DIAPH3 is linked to aggressive tumor behavior and may be involved in how these brain tumors grow.

Figure 1

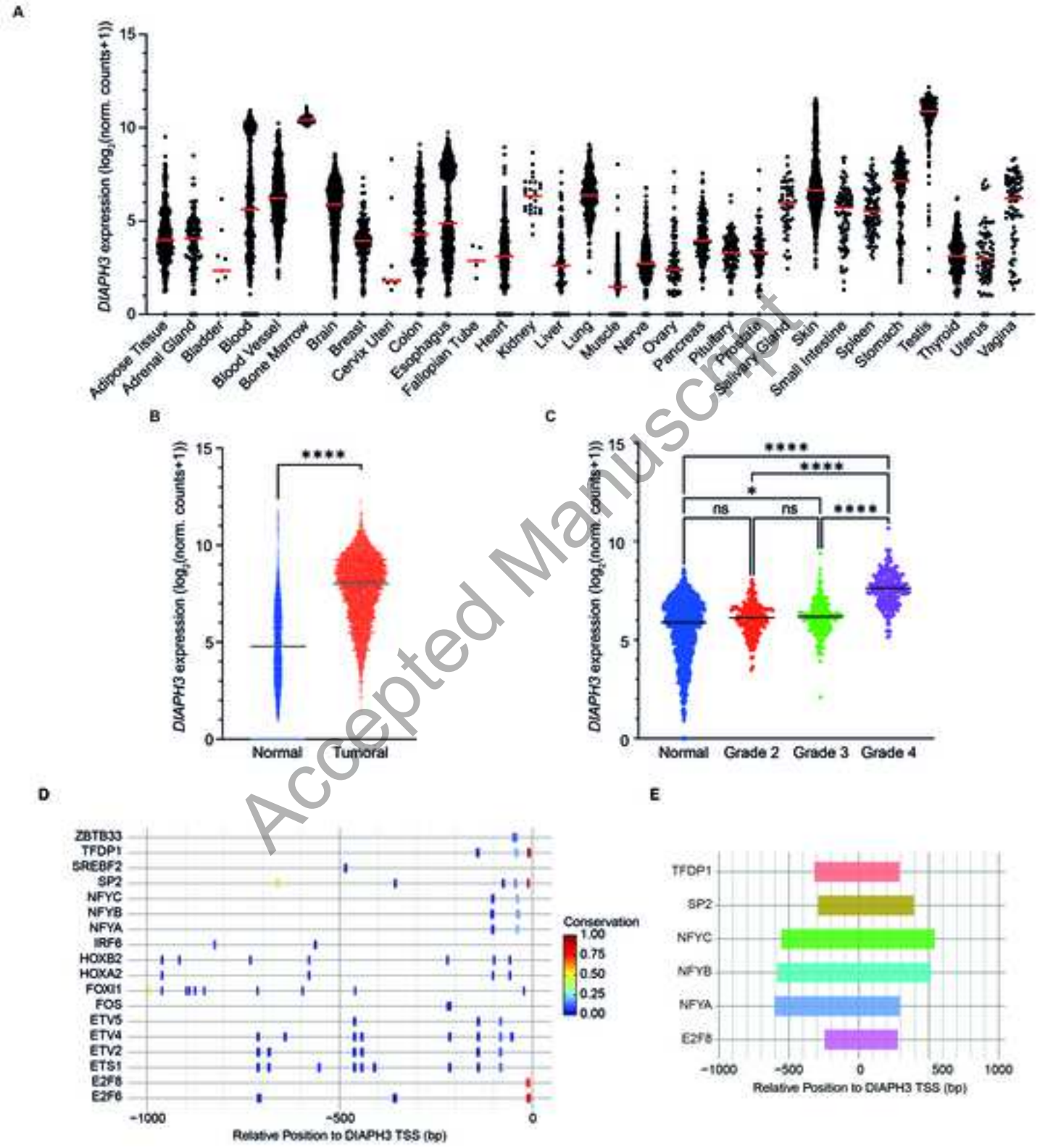

Figure 2

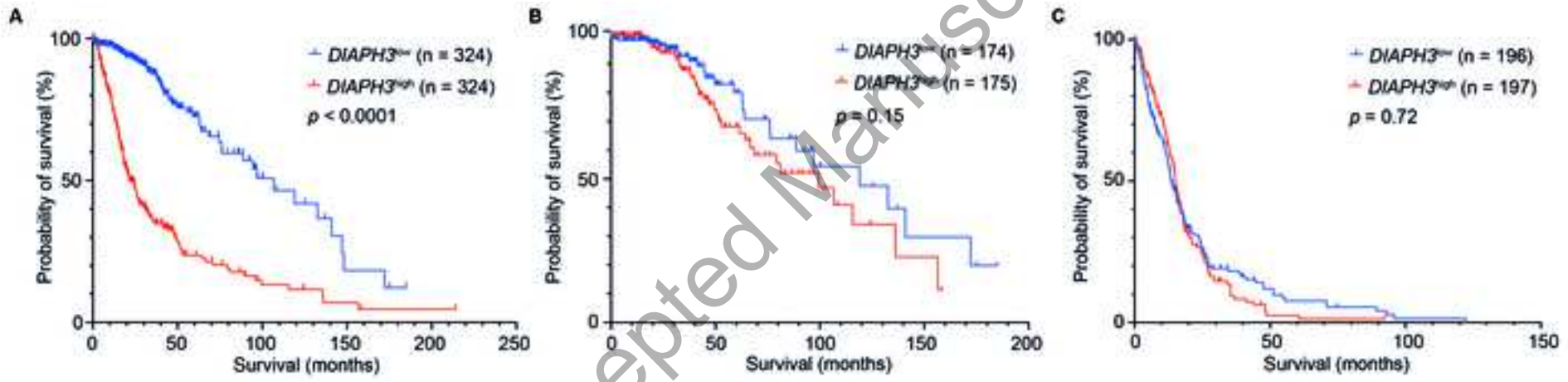

Figure 3

Click here to access/download;Figure;Fig3.tif

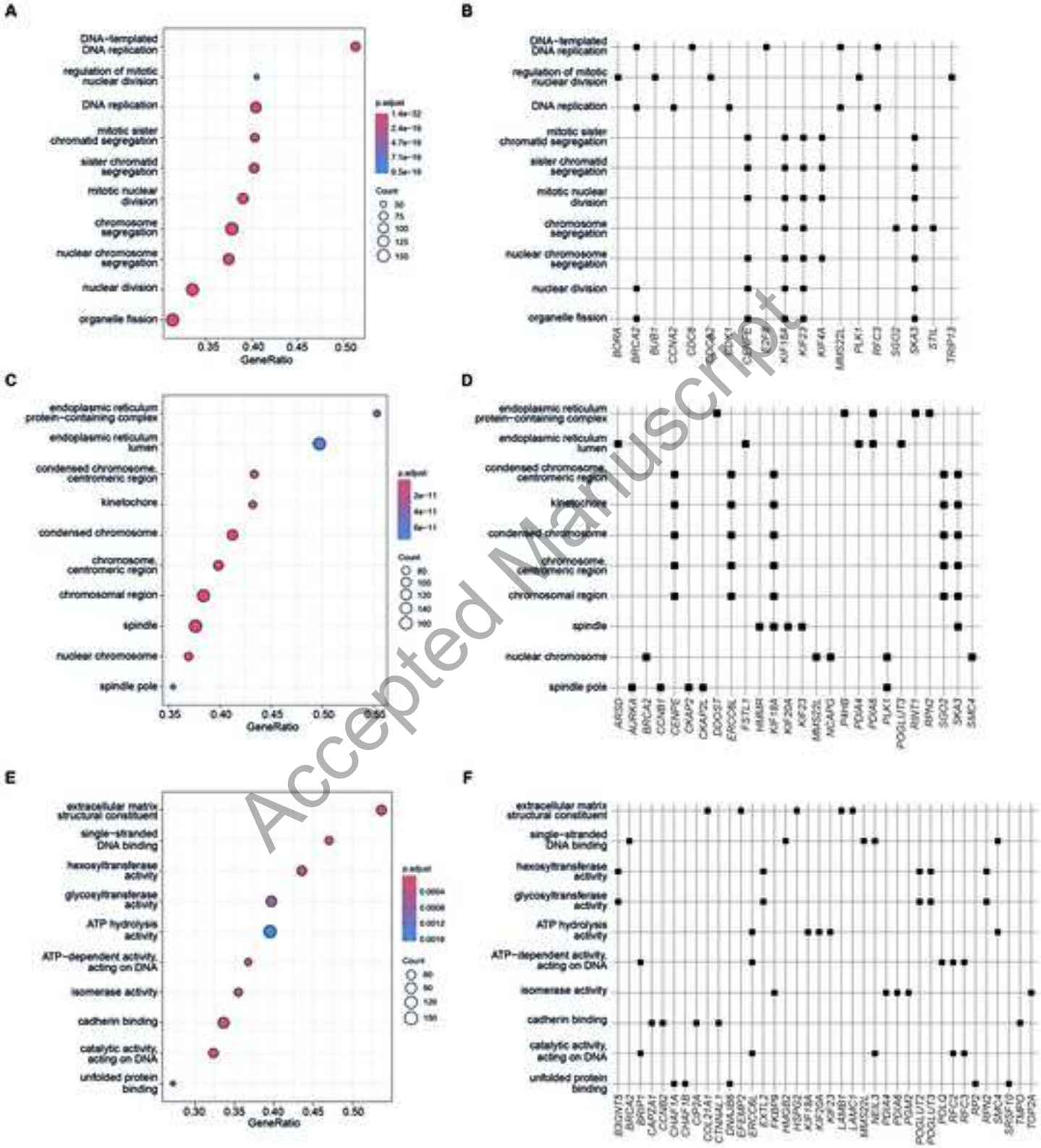

Figure 4

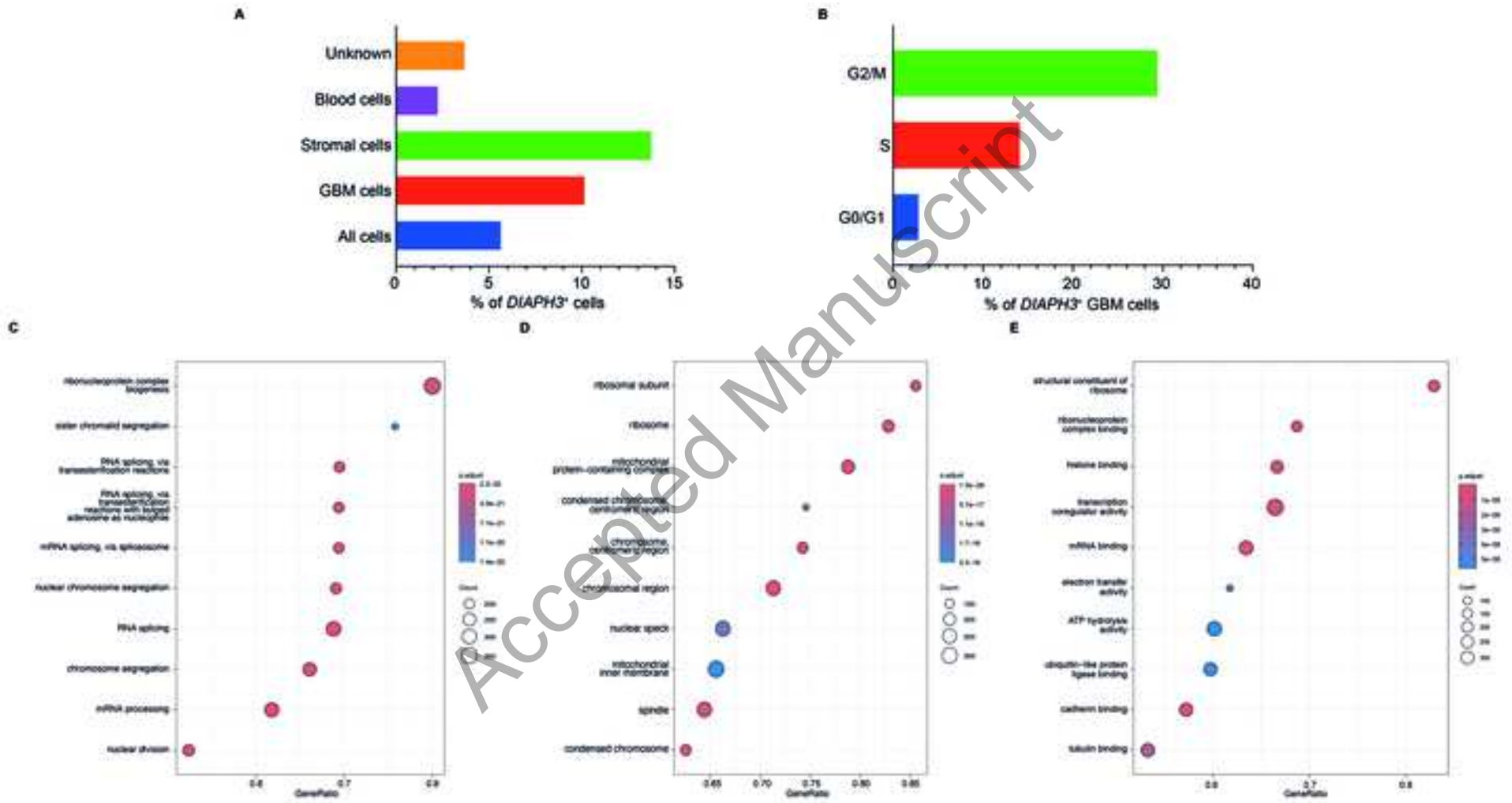

Figure 5